Sliding Mode Control with Fuzzy Adaptive Perturbation Compensator for 6-DOF Parallel Manipulator

Min Kyu Park
Graduate School of Intelligent Mechanical Engineering, Pusan National University, Gumjeong-ku, Busan 609-735, Korea
Min Cheol Lee*, Wan Suk Yoo
School of Mechanical Engineering, Pusan National University, Gumjeong-ku, Busan 609-735, Korea

This paper proposes a sliding mode controller with fuzzy adaptive perturbation compensator (FAPC) to get a good control performance and reduce the chatter. The proposed algorithm can reduce the chattering because the proposed fuzzy adaptive perturbation compensator compensates the perturbation terms. The compensator computes the control input for compensating unmodeled dynamic terms and disturbance by using the observer-based fuzzy adaptive network (FAN). The weighting parameters of the compensator are updated by on-line adaptive scheme in order to minimize the estimation error and the estimation velocity error of each actuator. Therefore, the combination of sliding mode control and fuzzy adaptive network gives the robust and intelligent routine to get a good control performance. To evaluate the control performance of the proposed approach, tracking control is experimentally carried out for the hydraulic motion platform which consists of a 6-DOF parallel manipulator.

Key Words : 6-DOF Parallel Manipulator, Sliding Mode Control, Fuzzy Adaptive Perturbation Compensator, Observer-Based Fuzzy Adaptive Network

1. Introduction

Sliding mode control (SMC) is very attractive method for nonlinear systems (Hashimoto et al., 1987 ; Lee et al., 1998 ; Slotine, 1983). It has been confirmed as an effective robust control approach for nonlinear systems against parameters and load variations. However, some bounds on system uncertainties must be estimated in order to guarantee the stability of the closed-loop system, and its implementation in practice has been caused an inherent chattering problem, which is undesirable in application. Several researchers have tried to reduce the tracking error and the inherent chatter by smoothing a switching action and by designing the perturbation compensator. In case of researches related with smoothing the switching action, an advanced sliding mode control algorithm with two dead zones and a saturation function was proposed for reducing the chattering (Lee et al., 1998). However, this algorithm could not completely reduce the inherent chattering caused by excessive switching inputs around the sliding surface. And, a fuzzy sliding mode control algorithm was designed to reduce the chatter by using the fuzzy rules (Choi and Kim, 1997).

The perturbation compensator is very effective method to reduce the inherent chatter without degrading the control performance (Slotine, 1984; Kim and Lee, 2000). A switching gain in SMC with perturbation compensator is much smaller than the gain in conventional SMC. Therefore, many researches have reported about the per-

* Corresponding Author,
E-mail : mclee@pusan.ac.kr
TEL : +82-51-510-2439; **FAX** : +82-51-512-9835
School of Mechanical Engineering, Pusan National University, Gumjeong-ku, Busan 609-735, Korea.
(Manuscript **Received** June 3, 2002; **Revised** February 9, 2004)

turbation compensator such as the time delay control (TDC), the disturbance observer (DOB), and so on (Elmali and Olgac, 1992; Hsia and Gao, 1990; Kim et al., 1996; Slotine et al., 1987; Youcef-Tomei and Ito, 1990). These conventional perturbation compensators have some problems. In case of the TDC, the full state feedback condition and accurate model of a system is required. It is really undesirable when the sensor signal includes the noise. Another approach, the DOB, is formulated with respect to the linear system and the low pass filter in frequency domain with output feedback condition. It is difficult to design an adequate cutoff frequency of filter. And, the adequate cutoff frequency has to be selected according to a characteristic of a system.

In order to overcome these difficulties this study proposes a new perturbation compensator with adaptive scheme. In many case, the perturbation components of a dynamic system are the source of tracking errors and velocity errors of a controlled system because the control law is designed to usually compensate the estimated model. The main idea of the new perturbation compensator is to minimize the estimation error and estimation velocity error by using an observer-based fuzzy adaptive network (FAN) with adaptive scheme. This perturbation compensator is called as a fuzzy adaptive perturbation compensator (FAPC) in this paper. And, the perturbation error dynamic is systematically derived and the dynamic equation is additionally attached to the perturbation compensator. This is called a residual perturbation compensator (RPC). It is expected that RPC could improve the performance of the perturbation compensator. As the proposed perturbation compensator is attached to the sliding mode control, an advanced sliding mode control scheme is proposed. The combination of sliding mode control and FAPC gives the robust and intelligent control routine to get a good control performance and reduce the chattering. System modeling is necessary to design the control algorithm. Therefore, simple model of the 6-DOF parallel manipulator including hydraulic actuators is derived by using virtual work principle, kinematic transform, linearization technique. Unknown linear elements such as equivalent mass and damping coefficient are estimated by using the signal compression method (Lee and Aoshima 1989; Park and Lee, 2002). Fig. 1 shows the developed 6-DOF parallel manipulator for a vehicle driving simulator (Park et. al., 2001). To evaluate the control performance of the proposed approach, tracking control is experimentally carried out for the 6-DOF parallel manipulator.

Fig. 1 6-DOF parallel manipulator for vehicle driving simulator

2. Modelling of 6-DOF Parallel Manipulator

2.1 Dynamic model of 6-DOF parallel manipulator

The 6-DOF motions are composed of linear and angular motions. The linear motions consist of longitudinal (surge), lateral (sway), and vertical (heave) motion. The angular motions are described by Bryant angles whose rotational sequences are x, y, and z axis. The coordinates are set by an inertial frame and the moving frame attached to the upper plate. Here, we denote q as the 6-DOF coordinate vector with surge (u), sway (v), heave (w), roll (α), pitch (β), and yaw (γ). This vector is presented by

$$q=[u,\ v,\ w,\ \alpha,\ \beta,\ \gamma] \tag{1}$$

Fig. 2 shows the coordinates and notations of

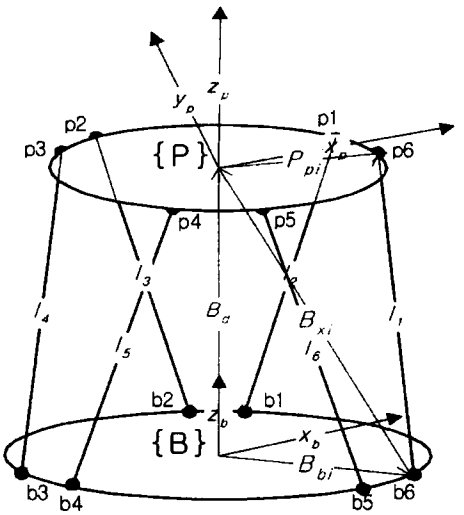

Fig. 2 Coordinate system of Stewart platform

the Stewart platform. The inertial frame $\{B\}(x_b, y_b, z_b)$ is fixed at the base plate, and the moving frame $\{P\}(x_p, y_p, z_p)$ at the upper plate. If the rotational transformation matrix and the linear vector are presented by ${}^P_B R$ and B_a, respectively, the length vector (x) of the ith joint is written as

$$x = B_{qi} = B_a - B_{bi} + {}^P_B R\, P_{pi} \tag{2}$$

where

$${}^P_B R = \begin{bmatrix} C_\beta C_\gamma & -S_\gamma C_\beta & S_\beta \\ C_\gamma S_\alpha S_\beta + C_\alpha S_\gamma & -S_\alpha S_\gamma S_\beta + C_\alpha C_\gamma & -S_\alpha C_\beta \\ -C_\gamma C_\alpha S_\beta + S_\alpha S_\gamma & C_\alpha S_\beta S_\gamma + S_\alpha S_\gamma & C_\alpha C_\beta \end{bmatrix}$$

The actuator lengths are computed by using the given position and orientation of the platform. This problem is called the inverse kinematics of a Stewart platform. The forward kinematics is the reverse of the inverse kinematics.

The forward kinematic problem is not easy to be solved, because the solution of this problem may be analytically presented as the roots of 16th or 40th order polynomial and not unique (Nair and Maddocks, 1994). Therefore, numerical method such as the Newton-Rhapson method is widely used in order to solve the forward kinematics.

The dynamic equation of the Stewart platform considering all inertia effect is known as being very difficult to derive. Lebret derived the dynamic equation using the Lagrange method and virtual work principle (Lebret et al., 1993). This equation can be written as

$$M_P(q)\ddot{q} + C_P(q, \dot{q})\dot{q} + G_P(q) = J^T U_P \tag{3}$$

where $M_P(q) \in R^{6\times6}$ is the inertia matrix. $C_P(q) \in R^{6\times6}$ corresponds to the centrifugal and Coriolis forces matrix. $G_P(q) \in R^{6\times1}$ is the gravity force vector. $J(q) \in R^{6\times6}$ is Jacobian matrix, and $U_P(q) \in R^{6\times1}$ is actuator force vector. After doing an algebraic operation such as $\dot{q} = J^{-1}\dot{x}$ and a kinematic transformation, Eq. (3) can be expressed as

$$\tilde{M}_P(q)\ddot{x} + \tilde{C}_P(q, \dot{q})\dot{x} + \tilde{G}_P(q) = U_P \tag{4}$$

where

$$\tilde{M}_P(q) = J^{-T}(q) M(q) J^{-1}(q)$$

$$\tilde{C}_P(q, \dot{q}) = J^{-T}(q) M(q) \frac{d}{dt} J^{-1}(q) + J^{-T}(q) C(q, \dot{q}) J^{-1}(q)$$

$$\tilde{G}_P(q) = J^{-T}(q) G(q)$$

where x is a vector of actuator length.

Next, the dynamics of actuator is considered. Assuming nonlinear part acts as a disturbance to the model, simple linear dynamics is obtained such as

$$M_A\ddot{x} + C_A\dot{x} + U_P = K_{SV} U_A \tag{5}$$

where M_A is the summation of equivalent masses of all of the translational part in the actuator. C_A is the equivalent damping coefficient. K_{SV} is a spool constant. Therefore, the nominal dynamic equation of the Stewart platform system including the manipulator and actuator dynamics becomes

$$M_T(q)\ddot{x} + C_T(q, \dot{q})\dot{x} + G_T(q) = K_{SV} U_A \tag{6}$$

where $M_T = \tilde{M}_P + M_A$, $C_T = \tilde{C}_P + C_A$, $G_T = \tilde{G}_P(q)$. After separating a linear element and a nonlinear element in Eq. (6), this equation can be re-expressed as

$$M_n\ddot{x} + C_n\dot{x} = K_{SV} U_A + \Psi \tag{7}$$

where M_n and C_n is the summation of all linear terms in M_T and C_T. The perturbation Ψ is composed of the summation of the nonlinear terms

among inertia moments, the Coriolis and centrifugal force, the gravity force, the friction force, and external disturbance.

2.2 Identification of 6-DOF parallel manipulator using signal compression method

It is difficult to apply an impulse signal to real system because the magnitude of the signal is infinite and the period is very short. To solve these problems, an equivalent impulse signal is generated by using the signal compression method (Lee and Aoshima, 1989; Park and Lee, 2002). The equivalent impulse signal called test signal has a flat power spectrum in a desired frequency range and a low amplitude. The signal is also lasted for a long time as shown in Fig. 3. Therefore, the test signal is able to be applied to a real system in order to estimate uncertain parameters.

To estimate uncertain parameters of the parallel manipulator as shown in Fig. 1, the test signal is supplied through the D/A converter. The length of the actuator according to the supplied test signal is detected by linear differential transducer and A/D converter. The output signal of actuator 1 is shown in Fig. 4. The output signal is changed into equivalent impulse responses through the FFT algorithm, the mathematical inverse phase-shift filter in the frequency domain, and IFFT. The element contributed by the nonlinear component is removed from the equivalent impulse response such as Fig. 5. As

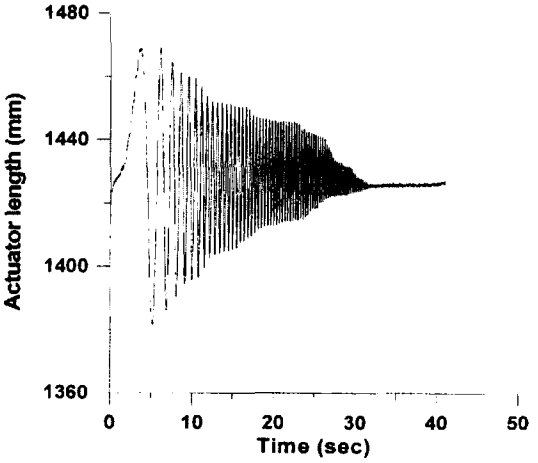

Fig. 4 Output signal of actuator 1

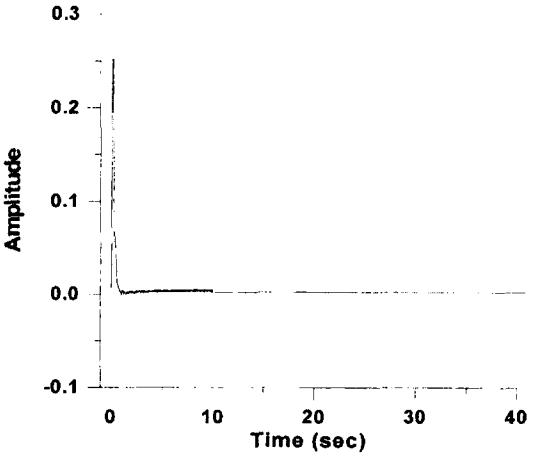

Fig. 5 Equivalent impulse response

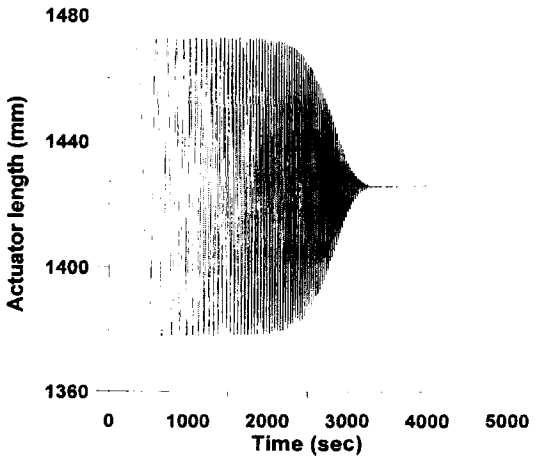

Fig. 3 Test signal

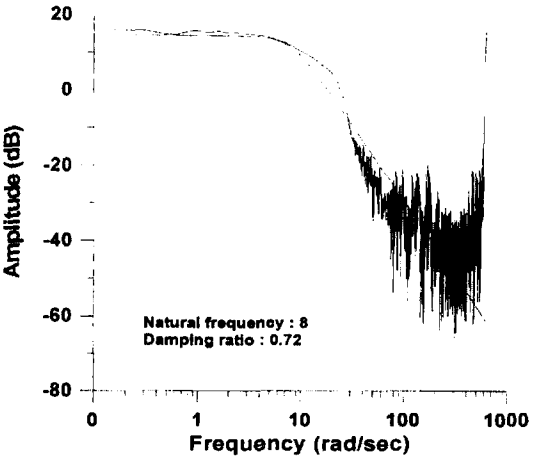

Fig. 6 Bode plot of actuator 1

comparing Bode plot of the transfer function from a model with that obtained from the equivalent impulse response, natural frequency (ω_n) and damping ratio (ζ) are estimated as shown in Fig. 6. Then, to estimate more exact values the cross-correlation between the equivalent impulse responses from an assumed model and a real system is used. The uncertain parameters such as natural frequency and damping ratio of 2nd order system are continuously renewed by when the obtained equivalent impulse response is closest to the impulse response from the assumed model. Finally the uncertain parameters are estimated when the cross-correlation is biggest. As these processes are applied to all actuators of the parallel manipulator, the natural frequency and damping coefficient of each actuator are obtained. Uncertain parameters (M_n, C_n) of Eq. (7) are obtained by the natural frequency and damping coefficient. The linear close-loop system of the parallel manipulator is expressed as

$$G_C(s)=\frac{L(s)}{U_A(s)}=\frac{K_pK_{SV}}{M_nS^2+C_nS+K_pK_{SV}} \tag{8}$$

where K_P is proportional control gain.

The linear close-loop system dynamics of the general mass-damper system is defined as follow :

$$G_C(s)=\frac{\omega_n^2}{s^2+2\zeta\omega_nS+\omega_n^2} \tag{9}$$

Therefore, the equivalent mass and damping coefficient of each actuator is calculated by

$$M_n=\frac{K_pK_{SV}}{\omega_n^2},\ C_n=2\zeta\sqrt{K_pK_{SV}M_n} \tag{10}$$

Table 1 Estimation results for parallel manipulator by using signal compression method

	Natural Frequency (rad/sec)	Damping Ratio	Cross Correlation	M_n(kg)	C_n(kg/s)
actuator 1	8	0.72	0.970	205.9	2372.7
actuator 2	7.6	0.74	0.975	228.2	2566.9
actuator 3	7.8	0.74	0.974	216.6	2501.1
actuator 4	8	0.74	0.973	205.9	2438.6
actuator 5	8	0.74	0.976	205.9	2438.6
actuator 6	8	0.76	0.976	205.9	2504.5

The estimated uncertain parameters are listed in Table 1.

3. Sliding Mode Control with Fuzzy Adaptive Perturbation Compensator

3.1 Sliding state observer

The sliding state observer is to drive the state of dynamic model toward a desired state in spite of the perturbation. It is assumed that the perturbations are bounded on upper limit by a known continuous function of the states. A sliding state observer for SISO system is a robust observer which estimates the state of a nonlinear system (Moura et al., 1997 ; Slotine et al., 1987). The nominal scalar model of the system is expressed as

$$M_{n,j}\dot{x}_j+C_{n,j}\dot{x}_j=u_j+\Psi_j \quad j=1,\ 2,\ 3,\ 4,\ 5,\ 6 \tag{11}$$

where $u_j(=K_{SV}U_A)$ is control input.

The actual perturbation Ψ_j may be divided into estimated and unknown residual perturbation as

$$\Psi_j(\boldsymbol{x})=\hat{\Psi}_j(\boldsymbol{x})+\Delta\Psi_j(\boldsymbol{x}) \tag{12}$$

where $\hat{\Psi}_j(\boldsymbol{x})$ is the estimated perturbation and $\Delta\Psi_j(\boldsymbol{x})$ is the unknown residual perturbation. The dynamic equation can be rewritten as

$$\ddot{x}_j=\frac{1}{M_{n,j}}(-C_{n,j}\dot{x}_j+u_j+\hat{\Psi}_j(\boldsymbol{x})+\Delta\Psi_j(\boldsymbol{x})) \tag{13}$$

The state space representation of a second order SISO system is as follows :

$$\begin{aligned}\dot{x}_{1j}&=x_{2j}\\ \dot{x}_{2j}&=-\frac{C_{n,j}}{M_{n,j}}x_{2j}+\frac{1}{M_{n,j}}\mu_j+\frac{1}{M_{n,j}}\Delta\Psi_j\end{aligned} \tag{14}$$

where $\mu_j=u_j+\hat{\Psi}_j$ is modified control input.

The sliding state observer is given by

$$\begin{aligned}\dot{\hat{x}}_{1j}&=\hat{x}_{2j}-k_{1j}sat(\tilde{x}_{1j})-\alpha_{1j}\tilde{x}_{1j}\\ \dot{\hat{x}}_{2j}&=-\frac{C_{n,j}}{M_{n,j}}\hat{x}_{2j}+\frac{1}{M_{n,j}}\mu_j\\ &\quad -k_{2j}sat(\tilde{x}_{1j})-\alpha_{2j}\tilde{x}_{1j}\end{aligned} \tag{15}$$

where k_{1j}, k_{2j}, α_{1j}, α_{2j} are positive number and $\tilde{x}_{1j}=\hat{x}_{1j}-x_{1j}$ is the estimation position error and the saturation function $sat(\tilde{x}_{1j})$ is defined as

$$sat(\tilde{x}_{1j})=\begin{cases}\tilde{x}_{1j}/|\tilde{x}_{1j}|, & \text{if } |\tilde{x}_{1j}|\geq\varepsilon_{oj}\\ \tilde{x}_{1j}/\varepsilon_{oj}, & \text{if } |\tilde{x}_{1j}|<\varepsilon_{oj}\end{cases}$$

where ε_{oj} is an observer constant as the boundary layer of sliding mode. Using Eqs. (14) and (15), the estimation error dynamics are

$$\begin{aligned}\dot{\tilde{x}}_{1j}&=\tilde{x}_{2j}-k_{1j}sat(\tilde{x}_{1j})-\alpha_{1j}x_{1j}\\ \dot{\tilde{x}}_{2j}&=-k_{2j}sat(\tilde{x}_{1j})-\alpha_{2j}\tilde{x}_{1j}-\frac{1}{M_{n,j}}\Delta\Psi_j\end{aligned} \tag{16}$$

where the uncertainty $\left(-\frac{C_{n,j}}{M_{n,j}}\tilde{x}_{2j}\right)$ is assumed to be part of the residual perturbation $\Delta\Psi_j$.

Fig. 7 shows the state space of the sliding state observer.

The sliding mode of the observer takes place on the line $\tilde{x}_{1j}=0$ of the state space as shown in Fig. 7. The conditions for the existence of sliding mode are as follows:

$$\begin{aligned}\tilde{x}_{2j}&\le(k_{1j}+\alpha_{1j}\tilde{x}_{1j}) \quad \text{if } \tilde{x}_{1j}>0\\ \tilde{x}_{2j}&\ge(-k_{1j}+\alpha_{1j}\tilde{x}_{1j}) \quad \text{if } \tilde{x}_{1j}<0\end{aligned} \tag{17}$$

Once the sliding takes place on the line to be $\tilde{x}_{1j}=0$ and $\dot{\tilde{x}}_{1j}=0$, the error dynamics from Eq. (16) is derived as

$$\dot{\tilde{x}}_{2j}+(k_{2j}/k_{1j})\tilde{x}_{2j}=-\frac{1}{M_{n,j}}\Delta\Psi_j \tag{18}$$

It is desirable to set the break point k_2/k_1 as high as possible in order to maximize the attenuation from $\Delta\Psi_j$ to $\tilde{x}_{2j}$.

The stability of the sliding state observer is guaranteed by setting as

$$k_{2j}\ge\left|\frac{1}{M_{n,j}}\Delta\Psi_j\right| \tag{19}$$

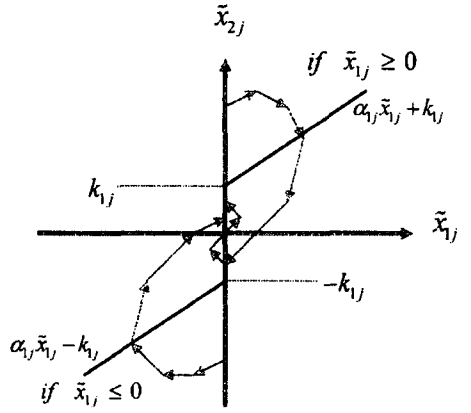

Fig. 7 State space of sliding state observer

The condition is derived as considering a steady-state of sliding mode ($|\tilde{x}_{2j}|\le k_{1j}$).

It means that estimation errors can be reduced by increasing k_2/k_1 in spite of $\Delta\Psi_j$. Therefore, the sliding state observer has robustness to the residual perturbation.

3.2 Sliding mode control

The estimated sliding function is defined as

$$\hat{s}_j=\dot{\hat{e}}_j+c_j\hat{e}_j \tag{20}$$

where c_j is the desired control bandwidth and always positive, $\hat{e}_j=\hat{x}_{1j}-x_{1dj}$ is the estimated position error and $[x_{1dj}\ \dot{x}_{1dj}]^T$ is the desired motion cue for the jth degree of freedom. The actual sliding function is presented by

$$s_j=\dot{e}_j+c_je_j \tag{21}$$

where $e_j(=x_{1j}-x_{1dj})$ is the actual position error.

The modified control input (μ_j) of Eq. (14) is selected by using time derivative of the Lyapunov function candidate be given by $\hat{s}_j\dot{\hat{s}}_j<0$ to satisfy the boundary layer attraction condition to generate sliding mode.

In case of SMC without state observer and perturbation compensator, the desired $\dot{s}_j$ for giving robustness on perturbation (Kim and Lee, 2000) is selected as follows:

$$\dot{s}_j=-K_j\,sat(s_j)+\frac{\Psi_j}{M_{n,j}} \tag{22}$$

where

$$K_j\ge\left|\frac{\Psi_j}{M_{n,j}}\right|$$

And, in case of SMC with perturbation compensator, a desired $\dot{s}_j$ for compensating the unknown residual perturbation must be selected as follows:

$$\dot{s}_j=-K_j\,sat(s_j)+\frac{\Delta\Psi_j}{M_j} \tag{23}$$

where

$$K_j\ge\left|\frac{\Delta\Psi_j}{M_{n,j}}\right|$$

However, in case of the sliding state observer based SMC with the perturbation compensator, a

desired $\hat{S}$ for satisfying the boundary layer attraction condition is selected as

$$\dot{\hat{s}}_j = -K_j\, sat(\hat{s}_j) - \left(\frac{k_{1j}}{\varepsilon_{oj}}\right)\tilde{x}_{2j} \tag{24}$$

where the state estimation error is bounded by $|\tilde{x}_{2j}| \le k_{1j}$, K_j has to be selected as $K_j \ge \frac{k_{1j}^2}{\varepsilon_{oj}}$ and $sat(\hat{s}_j)$ is defined as

$$sat(\hat{s}_j) = \begin{cases} \hat{s}_j/|\hat{s}_j|, & \text{if } |\hat{s}_j| \ge \varepsilon_{cj} \\ \hat{s}_j/\varepsilon_{cj}, & \text{if } |\hat{s}_j| < \varepsilon_{cj} \end{cases}$$

$sat(\hat{s}_j)$ is effectively used for anti-chattering problem. ε_{cj} is a constant as the boundary layer of sliding mode. The estimated sliding function is represented by using the sliding state observer equations of Eq. (15) and the estimation error dynamics of Eq. (16) as

$$\begin{aligned} \hat{s}_j = {} & \hat{x}_{2j} - k_{1j}\, sat(\tilde{x}_{1j}) - \alpha_{1j}\tilde{x}_{1j} \\ & - \dot{x}_{1dj} + c_j(\hat{x}_{1j} - x_{1dj}) \end{aligned} \tag{25}$$

It is assumed that x_{1j} and x_{2j} are perfectly known at time $t=0$. Therefore, all initial estimated state errors are zero. The observer starts on the sliding surface. And, if the gain k_{2j} was large enough, the estimated states always remain in the boundary layer (ε_{oj}) of the state observer. Therefore $sat(\tilde{x}_{1j})$ can be replaced by $\tilde{x}_{1j}/\varepsilon_{oj}$, Since the reaching phase is already eliminated, the attractivity terms, $\alpha_{1j}\tilde{x}_{1j}$ and $\alpha_{2j}\tilde{x}_{2j}$, are converge to zero. The assumed equations are arranged as follows :

$$sat(\tilde{x}_{1j}) = \tilde{x}_{1j}/\varepsilon_{oj},\ \alpha_{1j}\tilde{x}_{1j} \cong 0,\ \alpha_{2j}\tilde{x}_{2j} \cong 0 \tag{26}$$

Therefore, the estimated sliding function from Eq. (26) is arranged as

$$\hat{s}_j = \hat{x}_{2j} - (k_{1j}/\varepsilon_{oj})\,\tilde{x}_{1j} - \dot{x}_{1dj} + c_j(\hat{x}_{1j} - x_{1dj}) \tag{27}$$

The time derivative of the estimated sliding function is derived as

$$\dot{\hat{s}}_j = \dot{\hat{x}}_{2j} - (k_{1j}/\varepsilon_{oj})\,\dot{\tilde{x}}_{1j} - \ddot{x}_{1dj} + c_j(\dot{\hat{x}}_{1j} - \dot{x}_{1dj}) \tag{28}$$

Eq. (28) is re-written by using Eqs. (15), (16), and (26) as

$$\begin{aligned} \dot{\hat{s}}_j = {} & -\frac{C_{n,j}}{M_{n,j}}\hat{x}_{2j} + \frac{1}{M_{n,j}}\mu_j \\ & - [k_{2j}/\varepsilon_{oj} + c_j(k_{1j}/\varepsilon_{oj}) - (k_{1j}/\varepsilon_{oj})^2]\tilde{x}_{1j} \\ & - \ddot{x}_{1dj} + c_j(\hat{x}_{2j} - \dot{x}_{1dj}) \end{aligned} \tag{29}$$

Using Eqs. (24) and (29), it is possible to compute the modified control input of Eq. (14) as

$$\begin{aligned} \mu_j = M_{n,j}\Big\{ & \frac{C_{n,j}}{M_{n,j}}\hat{x}_{2j} - K_j\, sat(\hat{s}_j) \\ & + [k_{2j}/\varepsilon_{oj} + c_j(k_{1j}/\varepsilon_{oj}) - (k_{1j}/\varepsilon_{oj})^2]\tilde{x}_{1j} \\ & + \ddot{x}_{1dj} - c_j(\hat{x}_{2j} - \dot{x}_{1dj})\Big\} \end{aligned} \tag{30}$$

3.3 Fuzzy adaptive perturbation compensator

Our task is to use the FAN to approximate the perturbation function (Ψ) in Eq. (12), and proposes an adaptive control scheme to adjust the parameters of the FAN for minimizing the estimation error and estimation velocity error.

The fuzzy system consists of some fuzzy rules and a fuzzy inference system. The fuzzy inference system uses the fuzzy rules to perform a mapping from an input linguistic vector $z=[z_1\ z_2 \cdots\ z_n] \in R^n$ to an output linguistic variable $y \in R$. The ith fuzzy IF-THEN rule is written as Eq. (31) (Jamshidi et al., 1993).

$$\begin{aligned} R^{(i)}\text{: if } z_1 \text{ is } A_1^i \text{ and } z_2 \text{ is } A_2^i \text{ and } \cdots \\ z_n \text{ is } A_n^i \text{ then } y \text{ is } B^i \end{aligned} \tag{31}$$

where A_1^i, A_2^i, A_n^i, and B^i are fuzzy sets. The output is derived by the Takagi-Sugeno fuzzy model (Jang et al., 1997) :

First, ϕ_i is calculated by using product inference.

$$\phi_i = \Pi_{j=1}^{n}\mu_{A_j^i}(z_j) \tag{32}$$

Second, fuzzy basis value ($\bar{\phi}_i$) is obtained by using normalization process.

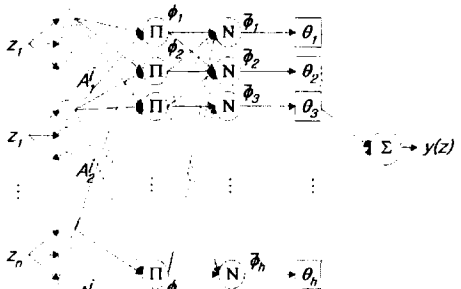

Fig. 8 Structure of observer based FAN

$$\bar{\phi}_i=\frac{\phi_i}{\sum_{i=1}^{h}\phi_i} \tag{33}$$

Finally, the output of fuzzy logic system can be obtained by

$$y(z)=\sum_{i=1}^{h}\theta_i\bar{\phi}_i=\boldsymbol{\theta}^T\bar{\boldsymbol{\phi}} \tag{34}$$

where $\mu_{A_j^i}(z_j)$ is membership function value of the fuzzy variable (z_j), h is the number of the total fuzzy IF-THEN rules, $\boldsymbol{\theta}^T=[\theta_1, \theta_2, \cdots, \theta_h]$ is adjustable parameter vector, and $\bar{\boldsymbol{\phi}}=[\bar{\phi}_1, \bar{\phi}_2, \cdots, \bar{\phi}_h]$ is fuzzy basis vector. The fuzzy logic approximator based on neural networks can be established. Fig. 8 shows the configuration of the FAN (Jang 1993).

This network has five layers. At layer 1, nodes represent the values of the membership function of total linguistic variables. Usually, bell-shaped membership function is widely used. Every node at layer 2, multiplies the incoming signals and sends the product result to the next layer. Every node at layer 3 calculates the fuzzy basis using normalization process. The ith node calculates the ratio of the ith rule's firing strength to the sum of all rules' firing strengths. At layer 4, every node including weighting factor (adjustable parameter) multiplies the fuzzy basis. At layer 5, the single node computes the overall output as the summation of all incoming signals.

Figure 9 shows the perturbation compensator using the observer based FAN. Input variables are the estimated position and velocity, and output variable is the estimated perturbation. The perturbation function is presented by

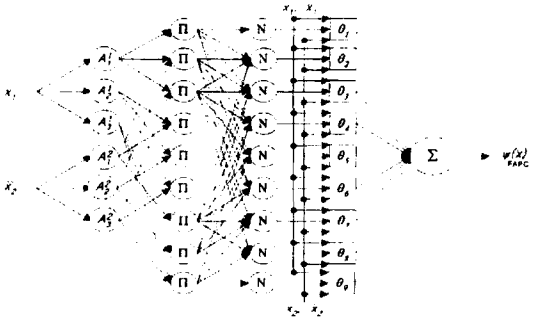

Fig. 9 Fuzzy adaptive perturbation compensator

$$\hat{\Psi}_{FAPC}(\hat{\boldsymbol{x}})=\boldsymbol{\theta}^T\bar{\boldsymbol{\phi}}(\hat{\boldsymbol{x}}) \tag{35}$$

In general, the simple projection algorithm is represented as

$$\dot{\boldsymbol{\theta}}=-\gamma\bar{\boldsymbol{\phi}}(\hat{\boldsymbol{x}})\,(\Psi-\hat{\Psi}_{FAPC}) \tag{36}$$

However, this scheme cannot directly apply because Ψ is unknown. In many case, the perturbation components of a dynamic system are the source of tracking errors and velocity errors of a controlled system because an estimated model without the perturbation is compensated by the conventional control law. Therefore, the main idea of the new perturbation compensator is to minimize the position and velocity errors as compensating the perturbation which is estimated by the observer-based fuzzy adaptive network with an adaptive scheme. The adaptive scheme is chosen as

$$\dot{\theta}=-\gamma(w_1\times\tilde{x}_1+w_2\times\tilde{x}_2)\,\bar{\boldsymbol{\phi}}(\hat{\boldsymbol{x}}) \tag{37}$$

where ω_1 and ω_2 are weighting factors, and γ is learning constant.

Substituting the control input $(u=\mu-\hat{\Psi})$ into the nominal dynamics Eq. (14), the following relationship is obtained as

$$M_{n,j}\ddot{x}+C_{n,j}\dot{x}-\mu_j=\Psi_j-\hat{\Psi}_{FAPC,j}=\Delta\Psi_j \tag{38}$$

where additional perturbation compensator $\hat{\Psi}_{RPC,j}$ is defined as

$$\hat{\Psi}_{RPC,j}\equiv M_{n,j}\ddot{\hat{x}}+C_{n,j}\dot{\hat{x}}-\mu_j \tag{39}$$

where $\hat{\Psi}_{RPC,j}$ is equivalent to the residual perturbation dynamics, and systematically derives from a nominal model of the system. This is called a residual perturbation compensator (RPC) in this paper. Therefore, the total pertur bation compensator is defined as

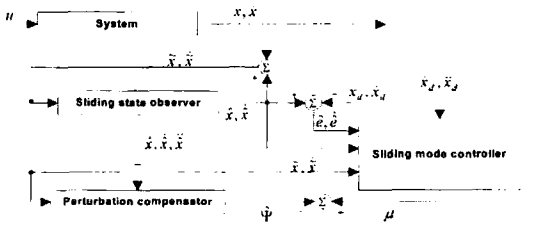

Fig. 10 Sliding mode control with the proposed perturbation compensator

$$\hat{\Psi}_j = \hat{\Psi}_{FAPC,j} + \hat{\Psi}_{RPC,j}$$

We expect that the residual perturbation ($\Delta\Psi_j$) converges to near zero by using the perturbation compensator. Namely, improving the performance of the perturbation compensator is expected.

The control input (u_j) is derived as

$$u_j = M_{n,j}\left\{ \frac{C_{n,j}}{M_{n,j}} \hat{x}_{2j} - K_j\, sat(\hat{s}_j) + [k_{2j}/\varepsilon_{oj} + c_j(k_{1j}/\varepsilon_{oj}) - (k_{1j}/\varepsilon_{oj})^2]\tilde{x}_{1j} + \ddot{x}_{1dj} - c_j(\hat{x}_{2j} - \dot{x}_{1dj}) \right\} - \hat{\Psi}_j \quad (40)$$

Fig. 10 shows the overall scheme of the sliding mode control with perturbation compensator.

4. Simulation And Experiment

A tracking control is performed to evaluate the tracking performance of the proposed control algorithm. The tuned sliding state observer parameters k_{1j}, k_{2j}, α_{1j}, α_{2j}, and ε_{oj} of Eq. (15) are 0.12, 2.4, 3, 5, and 0.002, respectively. And, the tuned control parameters c_j, K_j, and ε_{cj} of Eq. (40) are 20, 50, and 0.02, respectively. The parameters are selected by a trial and error method. The layer structure of perturbation compensator using the observer based FAN is a 2-6-9-9-1 as shown in Fig. 9. The input variables are an estimated actuator position and velocity and an output variable is the estimated perturbation. The observer based FAN has 6 membership functions which are the bell shapes as

$$\mu_{A_1^1} = 1/1 + [(\hat{x}_j + 1/0.5)^2]^{3.278}$$
$$\mu_{A_2^1} = 1/1 + [(\hat{x}_j/0.5)^2]^{3.278} \quad (41)$$
$$\mu_{A_3^1} = 1/1 + [(\hat{x}_j - 1/0.5)^2]^{3.278}$$

$$\mu_{A_1^2} = 1/1 + [(\dot{\hat{x}}_j + 1/0.5)^2]^{3.278}$$
$$\mu_{A_2^2} = 1/1 + [(\dot{\hat{x}}_j/0.5)^2]^{3.278} \quad (42)$$
$$\mu_{A_3^2} = 1/1 + [(\dot{\hat{x}}_j - 1/0.5)^2]^{3.278}$$

Input variables of the fuzzy adaptive perturbation compensator are a normalized estimated position and velocity. The range of values for these variables is from -1 to 1. And, a learning constant (γ) of Eq. (37) in on-line learning paradigm is set as 0.95. And the tuned weighting parameters (ω_1, ω_2) are 100 and 100, respectively. The payload of the Stewart platform is about 500 kg. The sampling time interval for control is selected by 10 msec. The reference position and velocity trajectory of each actuator are shown in Figs. 11 and 12, respectively. Figures 13 and 14 show the position and velocity error for each actuator when using the conventional sliding mode control as described (Slotine and Sastry, 1983).

$$u_j = -K_j\, sat(s_j) - c_j\dot{e}_j + \ddot{l}_{dj} \quad (43)$$

In spite of using the saturation function, the inherent chattering problem occurs in whole time, and the peak error is about -10 mm and not

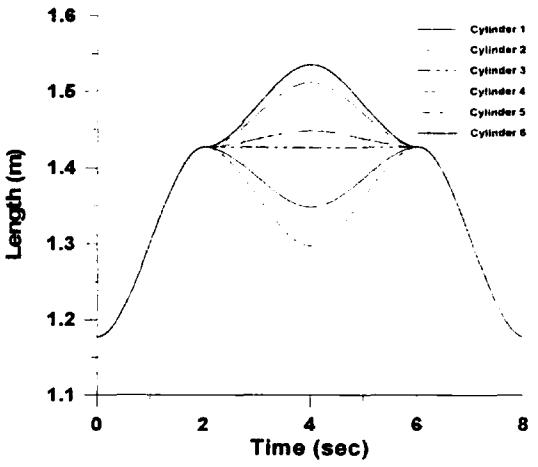

Fig. 11 Reference position trajectories

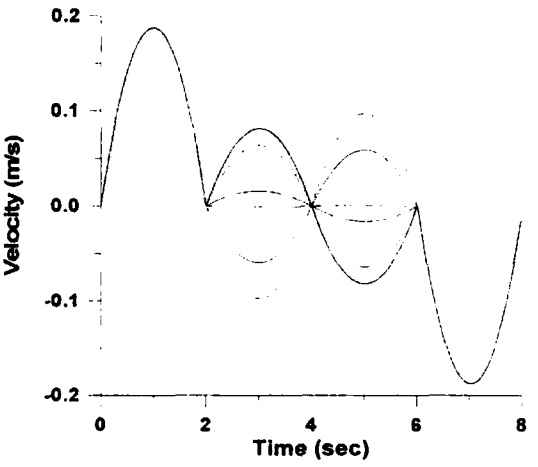

Fig. 12 Reference velocity trajectories

converged to zero. The simulation results of the proposed sliding control algorithm are shown in Figs. 15~Fig. 18. Figures 15 and 16 show the position error and velocity error for each actuator. Figure 17 shows the estimated position errors. Figures 15 and 16 show that the proposed perturbation compensator is rapidly converged to actual perturbation. Between 0 sec and 0.2 sec in Figs. 15 and 16, the peak position and velocity errors occur, because the estimated velocity error in Fig. 18 is so large for 0.1 sec. However, the estimated errors and velocity errors become much smaller, as the estimated perturbation values obtained by using the perturbation compensator are close to the actual perturbation values.

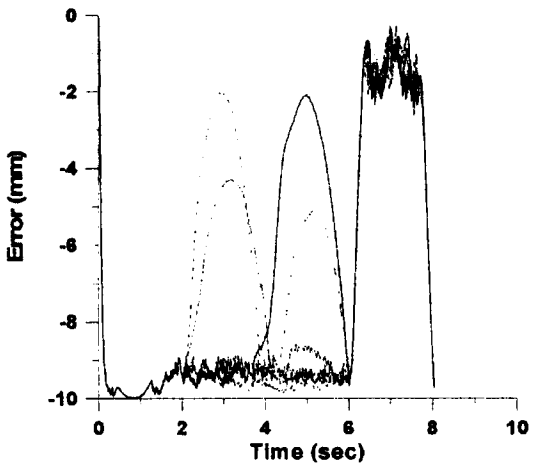

Fig. 13 Position errors in the conventional SMC

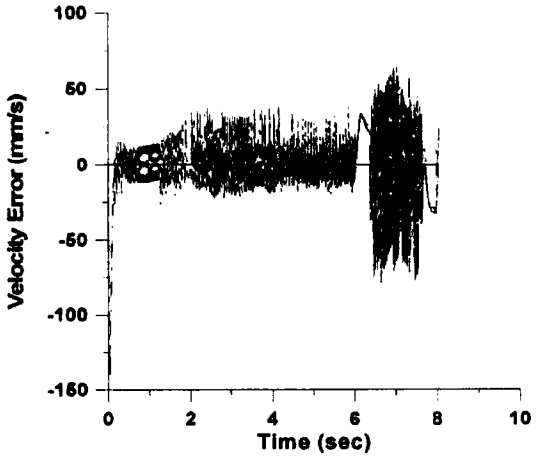

Fig. 14 Velocity errors in the conventional SMC

The results of the proposed SMC without compensating the residual perturbation $\hat{\Psi}_{RPC}$ are shown in Figs. 19 and 20. Figures 19 and 20 show the position errors and the compensated perturbation by using only fuzzy adaptive perturbation compensator, respectively. The perturbation compensator is converged after 0.4 sec. Therefore, the peak error occurs about −6.4 mm in initial state. It shows that the residual perturbation term acts on improving the converge rate and the estimated perturbation error.

Finally, performance of the perturbation compensator is evaluated by using the proposed com-

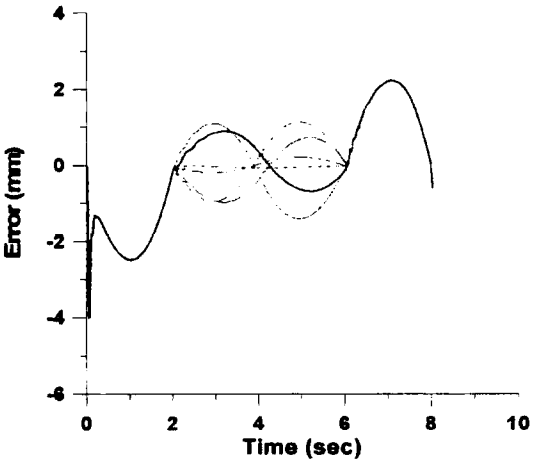

Fig. 15 Position errors in the proposed SMC+FAPC+RPC

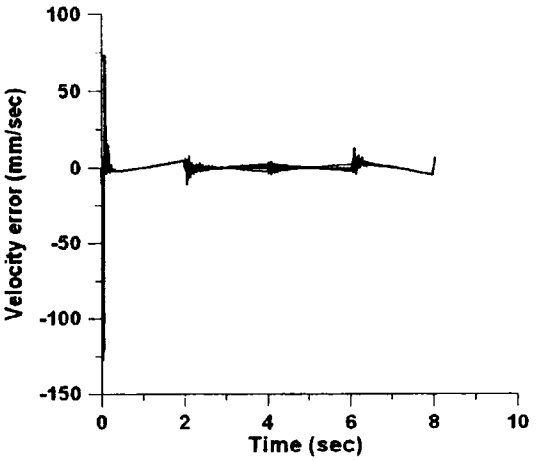

Fig. 16 Velocity errors in the proposed SMC+FAPC+RPC

pensator and conventional compensator. The conventional perturbation compensator based on the time delay control scheme is defined as

$$\begin{aligned}\hat{\Psi}(\boldsymbol{x}(t)) &= \Psi(\boldsymbol{x}(t-L)) \\ &= M_n\ddot{\boldsymbol{x}}(t-L)+C_n\dot{\boldsymbol{x}}(t-L)-\mu(t-L)\end{aligned} \tag{44}$$

where L is a sampling time of the digital controller and it is inevitable to adopt one step delayed signals to satisfy the causality.

The simulation results for actuator 1 are shown in Fig. 21. The proposed perturbation compensator is very fast and accurately converged to the actual perturbation. However, in case of the conventional perturbation compensator, the error of perturbation estimation is so large. Therefore, it is proved that the proposed compensator is valid.

Next, control performance is evaluated by experiment. The control board is composed of a microprocessor and peripheral circuits with a DIO (digital input and output), an ADC (analog to digital converter), a DAC (digital to analog converter), a serial communication circuit and timers. The micro-processor of the control board is the TMS320C31.

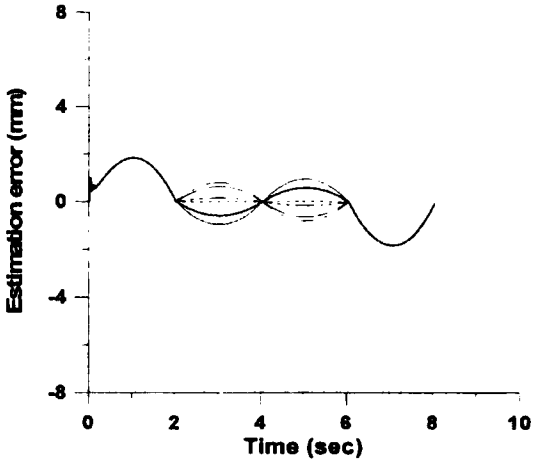

Fig. 17 Estimation position errors in the proposed SMC+FAPC+RPC

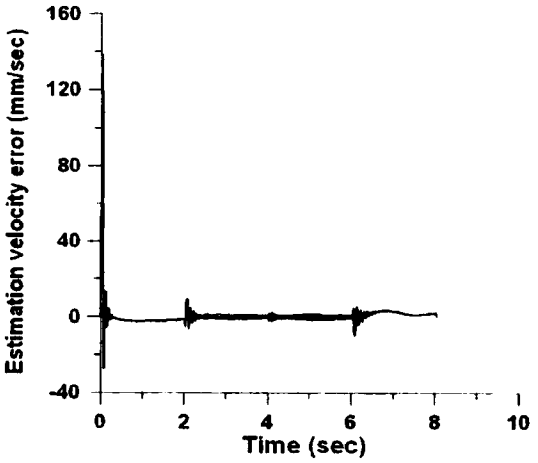

Fig. 18 Estimation velocity errors in the proposed SMC+FAPC+RPC

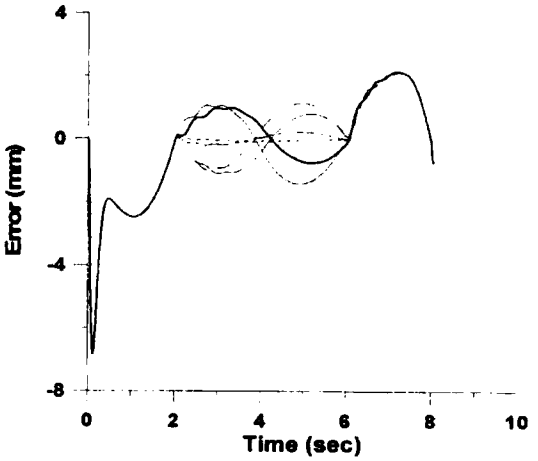

Fig. 19 Position errors in the proposed SMC+FAPC

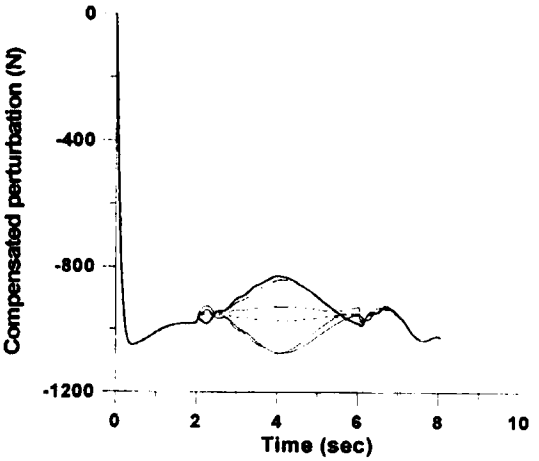

Fig. 20 Estimated perturbation by using FAPC

The experimental results are shown in Figs. 22~28. Figures 22 and 23 show position error and velocity error for each actuator, respectively. Figure 24 shows the estimated position errors. The compensated perturbation for each actuator are shown in Fig. 25. The estimated error is converged within 1.2 mm as shown in Fig. 24. And, the maximum position error is 3 mm. Figures 26 and 27 show the position errors and velocity errors by using the observer based sliding mode control without the perturbation compensator as described in Eq. (30), respectively. The position peak error is about 10 mm and not converged to zero. Control torques of actuator 1 from the observer based sliding mode control and the proposed control algorithm are presented by dotted line and solid line, respectively, in Fig 28. Comparing the results, the magnitude of the inherent chattering is substantially reduced by using the proposed control, whereas the chattering is seriously occurred in the observer based sliding mode control.

An inherent chattering occurred in the conventional sliding mode controller is reduced by using

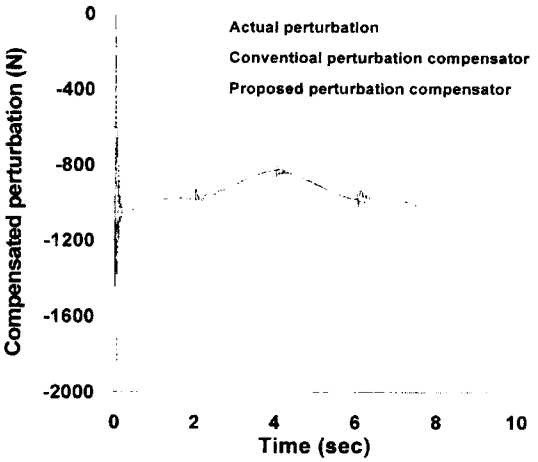

Fig. 21 Performance evaluation for perturbation compensators

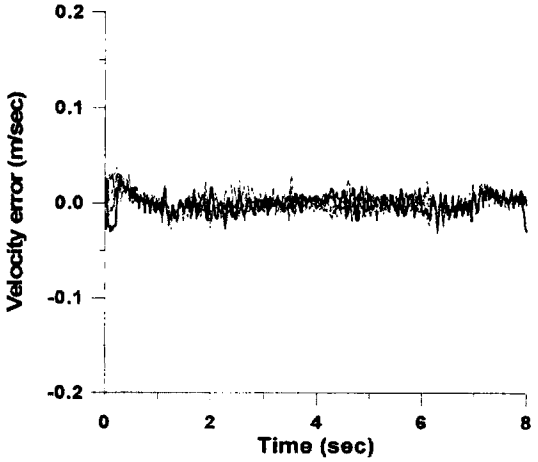

Fig. 23 Velocity errors in the proposed SMC+FAPC+RPC

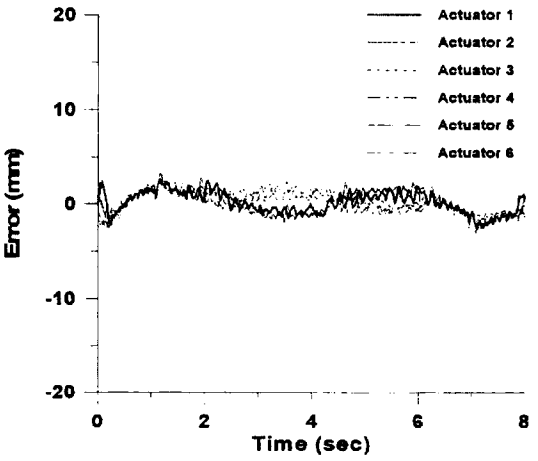

Fig. 22 Position errors in the proposed SMC+FAPC+RPC

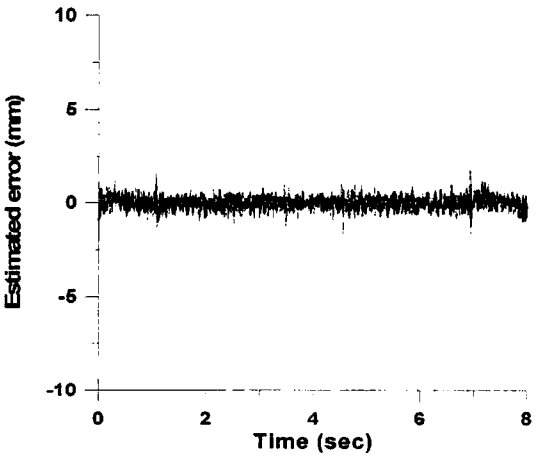

Fig. 24 Estimated position errors in the proposed SMC+FAPC+RPC

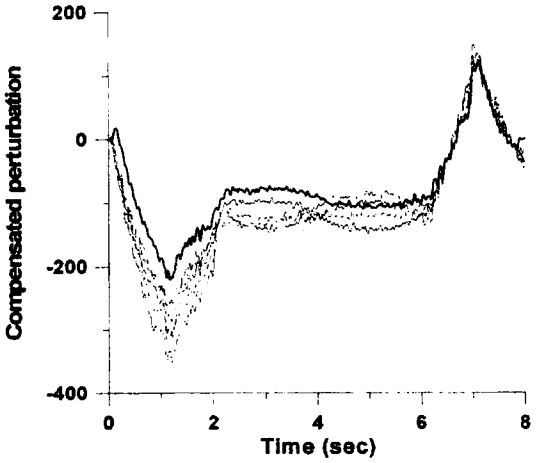

Fig. 25 Compensated perturbation by using FAPC+RPC

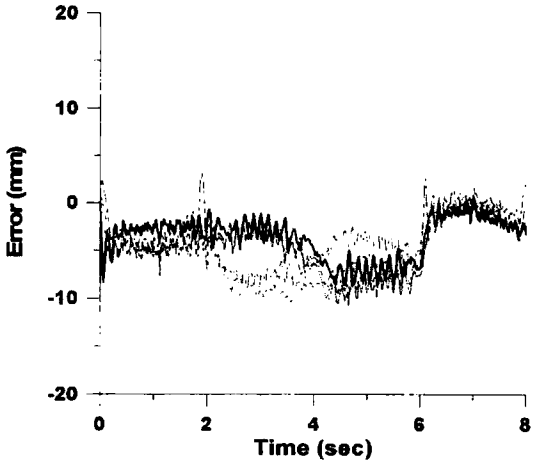

Fig. 26 Position errors by the observer based SMC

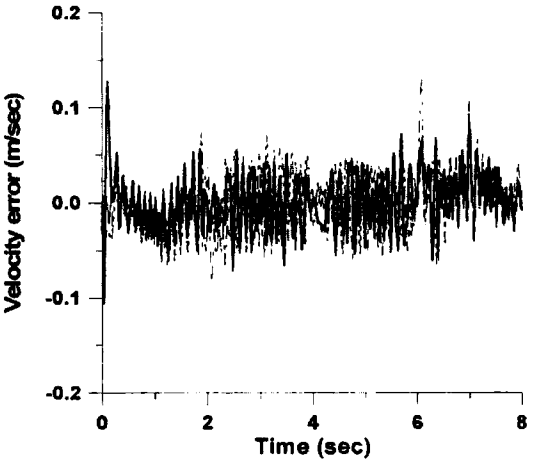

Fig. 27 Velocity errors by the observer based SMC

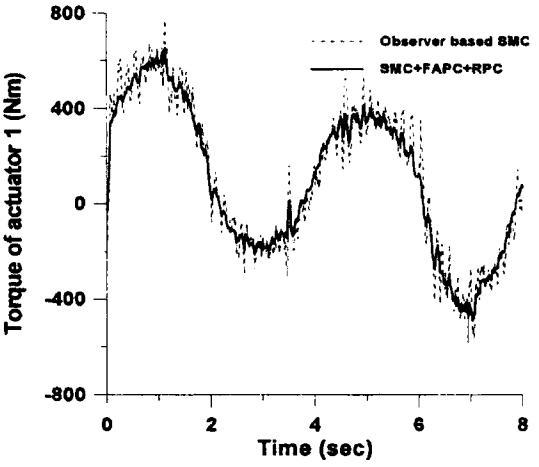

Fig. 28 Control torques of actuator 1

the sliding mode controller with perturbation compensator. It is verified that the performance of the proposed controller is a superior to the conventional sliding mode controller.

5. Conclusion

This paper proposed the sliding mode control with the perturbation compensator to reduce an inherent chattering and improve control performance. The nominal constant parameters of the system are identified by using the signal compression method. A dynamic uncertainty badly affected performance of a conventional compensator. In this paper, the new perturbation compensator was proposed using the fuzzy adaptive network and on-line learning scheme. The proposed perturbation compensator was fast and accurately converged into the actual perturbation as shown in simulation results. Finally, a tracking control simulation and experiment were carried out in order to evaluate the performance of the proposed control algorithm. The proposed control algorithm can reduce an inherent chattering as estimating the states and compensating a perturbation in accuracy. Therefore, the designed sliding mode control can provide reliable tracking performance.

Future work is to optimize the observer gains and control gains by using a pole assignment method and an optimization technique.

Acknowledgment

The authors would like to thank the Ministry of Science and Technology of Korea for its financial support through a grant (M1-0203-00-0017) under the NRL (National Research Laboratory) project.

References

Choi, S. B. and Kim, J. S., 1997, "A Fuzzy-Sliding Mode Controller for Robust Tracking of Robotic Manipulators," *Mechatronics*, Vol. 7, No. 2 pp. 199~216.

Elmali, H. and Olgac, N., 1992, "Sliding Mode Control with Perturbation Estimator: A New Approach," *International Journal of Control*, Vol. 56, No. 4, pp. 923~941.

Hashimoto, H., Maruyama, K. and Harashima, F., 1987, "A Microprocessor-Based Robot Manipulator Control with Sliding Mode," *IEEE Trans. Industrial Electronics*, Vol. 34, No. 1, pp. 11~18.

Hsia, T. C. and Gao, L. S., 1990, "Robot Manipulator Control using Decentralized Time-Invariant Time-Delayed Controller," *Proc. of IEEE International Conf. Robotics and Automation*, pp. 2070~2075.

Jamshidi, M., Vadiee, N. and Ress, T. J., 1993, Fuzzy Logic and Control, Prentice-Hall.

Jang, J. S. R., 1993, "ANFIS: Adaptive-Network-Based Fuzzy Inference System," *IEEE Trans. System, Man, And Cybernetics*, Vol. 23, No. 3, pp. 665~685.

Jang, J. S. R., Sun, C. T. and Mizutani, E., 1997, *Neuro-Fuzzy and Soft Computing*, Prentice-Hall.

Kim, N. I. and Lee, C. W., 2000, "Design of Sliding Mode Controller with Perturbation Estimation," *Transaction of KSME A*, Vol. 24, No. 4, pp. 866~873.

Kim, B. K., Chung, W. K. and Youm, Y. I., 1996, "Robust Learning Control for Robot Manipulators Based on Disturbance Observer," *Proceedings of the 1996 IEEE IECON*, Vol. 2, pp. 1276~1276.

Lebret, G., Liu, K. and Lewis, F. L., 1993, "Dynamic Analysis and Control of a Stewart Platform Manipulator," *Journal of Robotic Systems*, Vol. 10, No. 5, pp. 629~655.

Lee, M. C. and Aoshima, N., 1989, "Identification and Its evaluation of the System with a Nonlinear Element by Signal Compression Method," *Trans. of SICE*, Vol. 25, No. 7, pp. 729~736.

Lee, M. C., Son, K. and Lee, J. M., 1998, "Improving Tracking Performance of Industrial SCARA Robots Using a New Sliding Mode Control Algorithm," *KSME Int. J.*, Vol. 12, No. 5, pp. 761~772.

Moura, J. T., Elmall, H. and Olgac, N., 1997, "Sliding Mode Control with Sliding Perturbation Observer," *ASME Journal of Dynamics Systems, Measurement, and Control*, Vol. 119, pp. 657~665.

Nair, R. and Maddocks, J., 1994, "On the Forward Kinematics of Parallel Manipulators," *International Journal of Robotics Research*, Vol. 13, No. 2, pp. 171~188.

Park, M. K. and Lee, M. C., 2002, "Identification of Motion Platform Using the Signal Compression Method with Pre-Processor and Its Application to Sliding Mode Control," *KSME International Journal*, Vol. 16, No. 11, pp. 1379~1394.

Park, M. K., Lee, M. C., Yoo, K. S., Son, K., Yoo, W. S. and Han, M. C., 2001, "Development of the PNU Vehicle Driving Simulator and Its Performance Evaluation," *Proceeding of the 2001 IEEE International Conference on Robotics & Automation*, pp. 2325~2330.

Slotine, J. J., Hedrick, J. K. and Misawa, E. A., 1987, "On Sliding Observers for Non-Linear Systems," *ASME Journal of Dynamics Systems, Measurement, and Control*, Vol. 109, pp. 245~252.

Slotine, J. J. and Sastry, S. S., 1983, "Tracking Control of Non-linear Systems Using Sliding Surfaces with Application to Robot Manipulators," *International Journal of Control*, Vol. 38,

pp. 465~492.

Yang, S. Y., Lee, M. C., Lee, M. H. and Arimoto, S., 1998, "Measuring System for Development of Stroke-Sensing Cylinder for Automatic Excavator," *IEEE Trans. on Industrial Electronics*, Vol. 45, No. 3, pp. 376~384.

Youcef-Toumi, K. and Ito, O., 1990, "A Time Delay Controller Design for Systems with Unknown Dynamics," *ASME J. Dynamic Systems Measurement and Control*, Vol. 112, pp. 133~142.